Keysight Technologies
Imaging Graphene via Low Voltage Field Emission Scanning Electron Microscopy

Application Note

Introduction

Pursuing novel materials with intriguing properties is always an active field on the horizon of materials science. One paradigm is graphene which has attracted enormous passions and stimulated extensive research efforts all over the world since its discovery in 2004 [1]. With a monolayer of sp^2-bonded carbon atoms arranged in a honeycomb crystal lattice, graphene is a basic building block for all graphitic materials, from wrapping up into 0D fullerenes, or rolling into 1D nanotubes, to stacking into 3D graphite. For quite a long time, such a 2D graphitic layer had been described as a vintage model because this structure is not stable in theory [2]. The success of obtaining free-standing graphene, for the first time, by mechanical exfoliation of highly oriented pyrolytic graphite (HOPG) has immediately entranced both scientists in academia trying to understand the basic behavior of matter and those working in industry trying to explore novel applications. Predicted by theories and followed by experimental demonstrations, graphene possesses unique electrical, mechanical and optical properties. Currently graphene-based nanoelectronics are the subject of intense focus. For instance, the high intrinsic mobility in graphene makes it an attractive material for high-speed electronics [3], and its high optical transmittance coupled with high conductivity suggests graphene as an excellent transparent conductive electrode in flat panel displays, touch screens and cathode ray tubes [4]. In order for graphene to fulfill this promise in large-scale manufacturing of high-performance electronics, high-quality graphene with large dimensions is needed. Among several techniques for graphene synthesis, chemical vapor deposition (CVD) is the most promising approach for this purpose owing to the high quality of CVD graphene on large surface as well as the compatibility of CVD with current standard wafer-scale lithography and integrated circuit fabrication processes.

Characterization of graphene films is essential for the quality control purposes. Common techniques include optical microscopy, atomic force microscopy, Raman spectroscopy, transmission electron microscopy, Auger electron spectroscopy, etc. Scanning electron microscopy (SEM) is getting more popular for imaging graphene because it is a rapid, non-invasive and effective imaging technique which is complimentary to most other techniques. However, challenges still exist in SEM imaging of graphene films. To effectively image graphene, SEM needs to meet the following requirements:

1) High spatial resolution
Graphene films usually have nanoscale features. To resolve the morphology of graphene, a SEM must have a small beam spot size corresponding to a high spatial resolution.

2) Low beam energy
The ultra-thin graphene film is "transparent" to high energy electron beams. Since the preferred imaging information for SEM is the secondary electrons generated by the primary beam in the sample, low beam energy is required to image ultra-thin materials. Furthermore, low energy SEMs minimize beam induced sample damage and sample charging of exposed non-conducting materials, which is ideal for imaging graphene films on insulating substrates.

3) High contrast imaging
Many features in graphene are difficult to image because of poor contrasts. A perfect graphene monolayer is smooth and featureless making it a challenging surface for SEM imaging. A SEM with inherently high contrast and with the ability to enhance the contrast using multiple detection techniques is advantageous.

4) High performance detector
An efficient, high performance electron detector is required for detecting low energy electrons which provide the best surface contrast and topographic sensitivity.

Fortunately, the low voltage field emission scanning electron microscopy

(LV FE-SEM) can meet all the above requirements, hence it is potentially an ideal technique for graphene imaging.

In this study, different graphene samples were imaged by using a Keysight Technologies, Inc. 8500 compact FE-SEM. All samples were directly mounted on double carbon tapes without any other sample preparation followed by loading into the sample chamber for imaging. With an innovative miniature all-electrostatic electron beam column design, Keysight 8500 can achieve high resolutions at low beam voltages (500 V–2000 V). Its multi channel plate (MCP) detector sensitive to both secondary electrons (SE) and backscattered electrons (BSE) enables good image quality with high contrasts and excellent surfaced details making Keysight 8500 a good tool for studying graphene films. Images recorded at SE, BSE and topo modes will be presented which show detailed surface morphologies of graphene samples.

Resolving Morphologies of Graphene

1. As grown CVD graphene film
Graphene deposited on copper foil using chemical vapor deposition (CVD) is a very popular method to prepare samples [5]. The synthesis involves a catalytic decomposition of methane at a high temperature (~1000°C) in a low-pressure mixture of hydrogen followed by carbon deposition to form graphene films on copper substrates. This method is able to produce predominant single-layer graphene with a small percentage of multi-layers. It is presumed that the low solubility of carbon in Cu restrains the carbon deposition on the Cu surface only resulting in a single layer graphene film. Figure 1a shows typical features of the graphene film and the underlying Cu substrate. Both Cu grain boundaries (indicated as orange arrow heads) and Cu terracing with steps (indicated as green arrow heads) are apparent in the image. Those dark lines, indicated as cyan arrow heads, are characteristic graphene wrinkles which formed during the graphene film growth caused by its
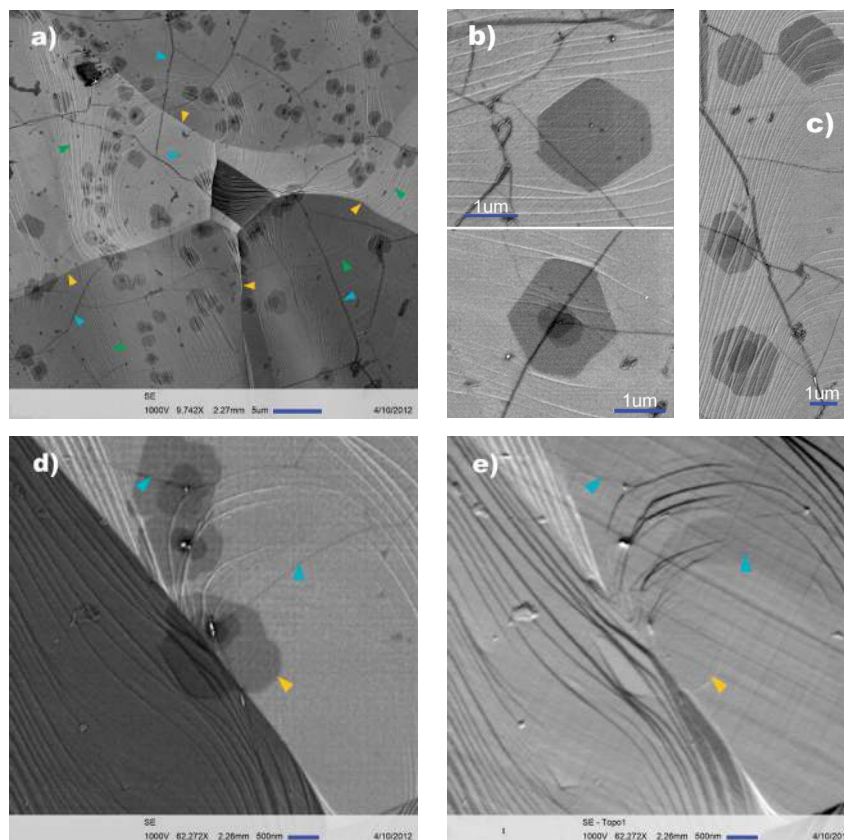

Figure 1. a) An overview image of CVD graphene film on Cu foil showing features; b) some bilayer graphene domains showing a hexagonal shape; c) all hexagonal domains show roughly the same orientation; d) SE image at a high magnification; e) corresponding topo image giving topographic information.

thermal expansion mismatch with Cu. The observation of graphene wrinkles crossing Cu boundaries and steps indicates the continuity of the graphene film all over the substrate. So the background in rather uniform brightness within individual Cu grains is actually the graphene monolayer. Another prominent feature is the darker flakes with a variety of shapes and dimensions which are attributed to multi-layer graphene domains. A possible contrast mechanism in SEM images for different numbers of graphene layers was described as the attenuation of secondary electrons from the substrate by graphene layers [6], which is similar to the contrast formation in Auger electron spectroscopy [7]. It can be seen from Figure 1a that most multi-layer domains are not in a regular shape and some have a second, third or fourth layer of smaller areas inside the domains. Nevertheless we still observed a number of flakes with some propensity of 6-fold domains. Figure 1b shows two domains in a regular hexagonal shape with well-identifiable 120° corners: one

is bilayer domain and the other one has bilayer, trilayer and quadrilayer domains. A perfect graphene multi-layer domain has the zigzag termination which was confirmed by Raman D band map [8]. The formation of such hexagonal domains is associated with the etching role of hydrogen gas involved in the CVD process. Figure 1c unveils an interesting phenomenon: four hexagonal bilayer domains have a roughly identical orientation within the same underlying graphene monolayer grain. This could be explained as the AB Bernal stacking of the bilayer graphene, where half of the carbon atoms in the second layer sit on top of the empty centers of hexagons in the first layer [9].

Figure 1d and 1e are a SE image and its corresponding topo image at a high magnification, respectively. Compared with the SE image, the topo image reveals the Cu terrace more obviously due to its enhanced signal in Z-direction. The narrow dark wrinkles (cyan arrow heads), which consist of a couple of graphene layers, still can be discerned in

the topo image indicating the tiny height difference related to the graphene monolayer. The topo image can barely differentiate the multi-layer domains from the monolayer which are obvious in the SE image. This is reasonable because the thickness difference of ~0.35 nm is beyond the capability of the SEM. As indicated by the orange arrow head, perceptibility of the bilayer edge in the topo image is most probably caused by the coincidence edge of a Cu step and the bilayer graphene.

2. Transferred graphene film

CVD has proven to be effective to grow large area graphene films in a good quality on metal substrates such as nickel, iridium, ruthenium, platinum and copper. However, when integrated in electronic devices, the graphene film must be electrically isolated from its surrounding environment and integrated onto a device-compatible substrate [10]. Hence efforts have been made to synthesize graphene layers directly on dielectric substrates such as quartz [11], regular SiO_2 [12], SiC [13], MgO [14], etc. Despite some successes, this CVD synthesis of graphene on dielectric substrates generally suffers from incomplete decomposition of the carbon precursor leading to a low crystalline quality and lots of structural defects. Therefore, techniques to transfer CVD grown graphene films from metal substrates to other substrates have been developed and are widely used because of its straightforward operation and low cost process [15]. From the device performance point of view, it is crucial to ensure that the quality of the graphene film does not degrade during the transfer process. However, in practical, this process usually generates contaminations or introduces structural defects including folds, cracks and holes which substantially affect the electrical behavior of the transferred graphene films. For example, the trapped contaminants may act as scattering centers and degrade the carrier transport performance of graphene film. LV FE-SEM is a powerful approach to check such defects at both micro and nanoscales which may not be observable by optical microscopy.

Here samples for imaging include three graphene films transferred to SiO_2/Si substrates by three different methods (Method 1, Method 2 and Method 3) which were modified from the commonly used PMMA-based transfer-printing method (unpublished results). The typical morphology of the first sample is shown in Figure 2a. Figure 2b, a topographic image of the same sample at a high magnification, clearly reveals a highly corrugated structure. It was reported that by using a SEM equipped with an in-lens SE detector, this rippled structure can be observed, whereas imaging this type of surface details is not possible when using a conventional Everhart-Thorney (ET) detector [11]. The in-lens detector is able to efficiently collect low-energy secondary electrons and in particular the SE1 signals which provide the highest resolution surface information. This is a critical capability as the ultrathin graphene can only be imaged using a low energy beam. The four quadrant MCP detector standard on the Keysight 8500 is proven to have good low beam energy performance which is comparable to in-lens detectors in other FE-SEMs.
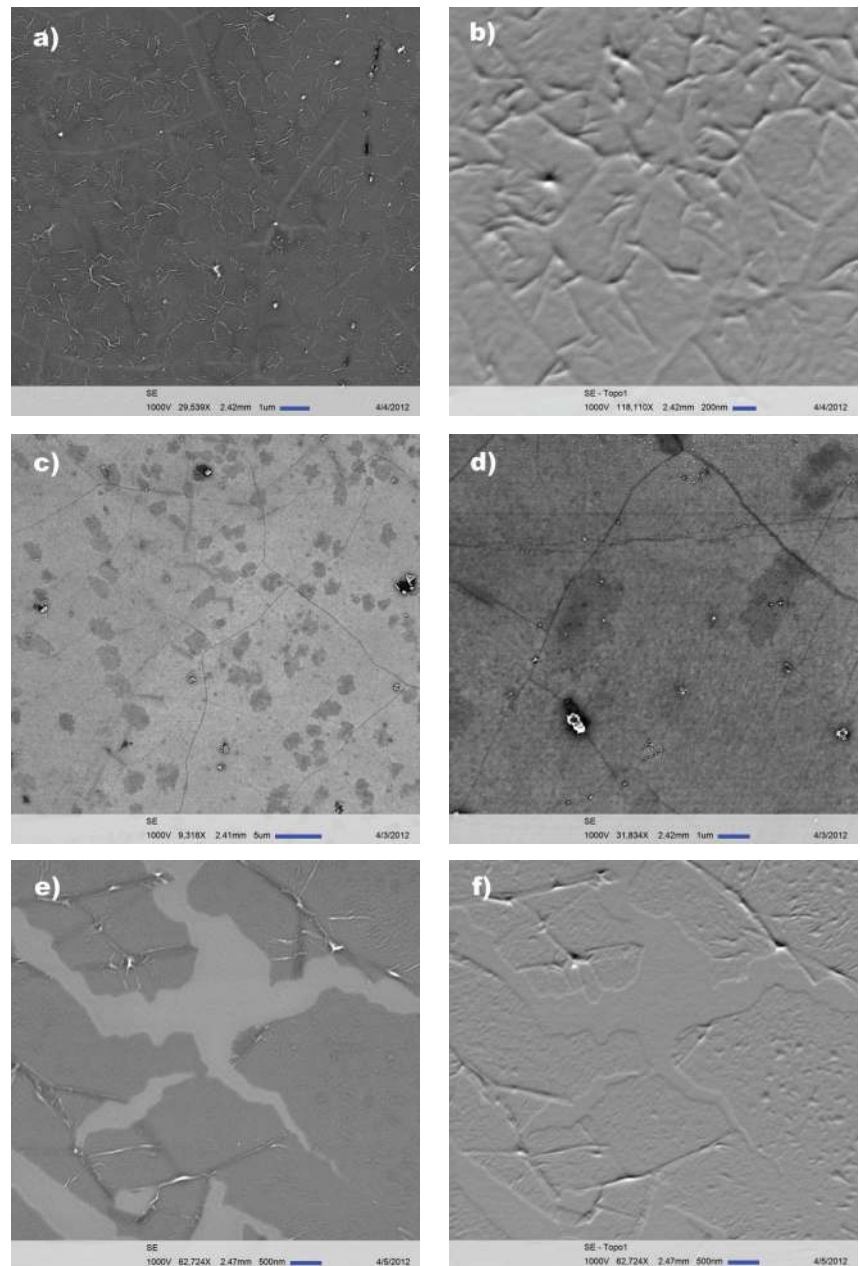

Figure 2. Graphene films transferred on SiO_2/Si substrate by three different methods. a) and b) highly corrugated morphology of the graphene film by Method 1; c) and d) continuous graphene film by Method 2; e) and f) cracked graphene film by Method 3.

This rippled structure is typical for transferred graphene films. As can be seen from Figure 1, the surface of Cu undergoes a significant reconstruction at high temperatures and tends to be rough with steps. As the growth of graphene film follows the surface of the underlying substrate, the as grown film is not flat at all. When it is removed from the "rough" Cu surface and released on a flat substrate, the graphene film cannot make a full contact with the substrate resulting in this ridge-like structure. It was hypothesized that water between the graphene layer and the substrate creates surface tension during the drying process which will drag the film into contact with the substrate [16]. It is also noticed that the dark lines, graphene wrinkles, are hardly observable. Figure 2c and 2d gives some surface information about the second sample. Differently, this transferred graphene film appears much smoother without any ripples. And both multi-layer domains and graphene wrinkles are preserved indicating a better transfer process. The image at a higher magnification, Figure 2d, also shows some impurity particles which may come from CVD itself [16] and some texture on the monolayer which could be the polymer residue. The third transfer method appears to bring many cracks to the film, as can be seen in Figure 2e. Ripples and surface roughness of graphene film are obvious in the topo image (Figure 2f). Apparently, most contour lines of graphene pieces match with neighbors suggesting a whole piece before cracking. It is believed that this unfavorable tear or cracking occurs during water evaporation in the transfer process. One feature observed from Figure 2e is the bright line along all the edges which could be caused by a combination of morphologic contrast and electron beam induced current flowing at the edge vicinity.

3. Graphene flakes

Non-uniform graphene flakes form when a whole graphene film breaks into small pieces. This usually happened in a bad transfer of graphene films. Figure 3a exhibits the morphology of graphene flakes after transfer from Cu foil used in CVD to another Cu
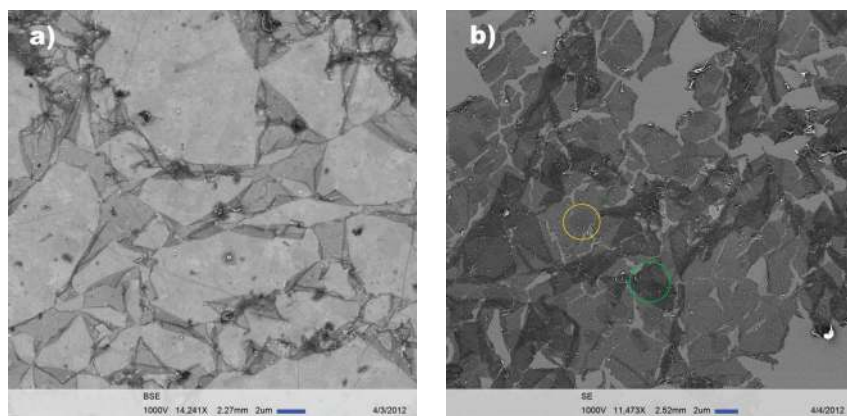

Figure 3. a) Non-uniform graphene flakes with curvature structures sitting on a Cu substrate; b) graphene flakes adhere to a Al_2O_3 substrate showing different gray-level contrasts which are attributed to multilayer domains (in the yellow circle) and multiple stacked films (in the green circle).

substrate. Apparently, small graphene pieces are separated and their edges seem to fold back due to their partially release from the target substrate. Less than ~15% of the graphene area is estimated to attach to the substrate which implies a weak contact between them. Another collection of graphene flakes displaying a different morphology is shown in Figure 3b. After transferred to an Al_2O_3 substrate, it seems most graphene flakes attach to the surface. Very dark areas were observed, as indicated in a green circle. This dark contrast cannot be assigned to a multi-layer graphene domain. It must be caused by a physical stacking of multiple graphene films instead. It is most likely that during the transfer, some flake pieces were completely released and resided on other graphene films. A multilayer graphene domain should display a weaker gray-level contrast, as shown in the yellow circle. A careful image interpretation is needed to identify the true morphology of graphene flakes so that the formation of non-uniform graphene flakes can be explained by considering the whole transfer process.

4. Graphene ribbons and carbon nanoscrolls

Graphene films with special morphologies were also observed under the LV FE-SEM. Figure 4a and 4b are SE and topo images of a graphene ribbon on a SiO_2/Si substrate, respectively. The ribbon shown here seems to have smooth and rather straight edges in parallel which possibly represent a well-defined zigzag or armchair

structure. Bright spots on the graphene ribbon are likely impurity nanoparticles with 20–30 nm in diameter which were introduced during the transfer process. These nanoparticles are so bright in SE imaging that the graphene ribbon shows pretty weak relative contrast. The topo image which highlights topographical variations reveals enhanced surface details. From Figure 4b, even the folding history of the ribbon can be envisioned. The possible cracking of a graphene film along certain crystalline directions could cause the formation of such ribbon-like structures. The observed graphene ribbon here has an average width of ~1 μm which is much larger than that of previously reported graphene nanoribbons [17]. Nanoribbons with narrow widths (<~10 nm) are predicted to exhibit extraordinary electrical properties which are promising for high performance transistors working at room temperature.

An interesting carbon nanomaterial, a carbon nanoscroll, is a two-dimensional graphene sheet spirally wrapped into a tubular structure. The unique properties of carbon nanoscrolls include the $\pi-\pi$ interaction between the inner and outer walls, and electric current flowing within the scrolled graphene layer [18]. The intrinsic rippled structure of transferred graphene films on substrates are fragile and easily tear or crack. It was found that the edge of a highly corrugated graphene film always folds back and scrolls into a tubular structure [16]. One carbon nanoscroll (blue arrow) is shown in Figure 4c. The driving force for nanoscroll formation is

the $\pi-\pi$ interaction of the overlapped parts which leads to a decreased total free energy of graphene [19]. In this case, the graphene film cracked due to the surface tension of water entrapped in the gaps between the graphene and the substrate in the drying process. After drying, the edge of the cracked graphene film became detached from the substrate and rolled up to from a carbon nanoscroll with a decreased total free energy. The pink arrow in Figure 4c indicates the polymer residue after the detachment of the graphene film. This residue is more obvious in the topo image, Figure 4d.

Effect of Electron Beam Voltages

The beam voltage determines the energy of electrons in the primary beam when they hit the specimen surface. A complex interaction between the incident beam and specimen atoms generates secondary electrons which may escape from the surface and be collected for the SE imaging. The beam energy not only affects the size of the interaction volume which is related to

the spatial resolution, but also affects the secondary electron yield. Generally, low voltage SEM refers to imaging at a beam voltage less than 5 kV. At low voltages, the low energy incident electron beam creates a substantially reduced interaction volume with penetration depths comparable to the escape depth of the SEs. In this case, the resolution is determined largely by the spot size of the beam and most of the information from the sample comes from within the SE escape depth. Consequently, LV FE-SEM is capable of high resolution and is highly sensitive to surface topography. To demonstrate the effect of beam voltages on SE imaging, we varied the beam voltage when imaging CVD grown graphene film on Cu foil. No charging effect needs to be considered due to the good conductivity of Cu foil.

Figure 5a–b, 5d–e, and 5g–h were obtained at the beam voltage of 550 V, 1000 V, and 2000 V, respectively. For comparison purpose, Figure 5a, 5d, and 5g show the same area, so do Figure 5b, 5e, and 5h. For an easy comparison, no signal intensity adjustment was applied on these images. The images

show that a 1000 V beam provides the best resolution. The topographic detail increases as the beam voltage is lowered. For instance, multi-layer domains (a yellow arrow head) consisting of bilayer, trilayer and quadrilayer, can be seen in different contrasts from Figure 5a, 5d and 5g. It is obvious that Figure 5a shows the highest contrast between different graphene layers while Figure 5g shows the lowest. Figure 5b, 5e and 5h show multilayer domains on Cu grain boundaries. Imaging at a higher beam energy generates a higher topographic contrast for the Cu boundaries. However, this unfavorable high contrast for unleveled Cu grains in Figure 5h obscures the surface details of the multilayer domains (magenta arrow head). By comparison, imaging at 550 V clearly exhibits the graphene flake with good contrast. It is believed that the enhanced thickness contrast at a lower energy is caused by a more sufficient attenuation of secondary electrons by the graphene layers. Monte Carlo simulation was conducted to compare the interaction between incident beams at different energies and the specimen [20]. In the simulation, we set the beam spot size as 10 nm, and the thickness of graphene on Cu substrate as 1.0 nm roughly corresponding to that of a trilayer graphene. The simulation results of electron beam energies of 550 V, 1000 V and 2000 V are shown in Figure 5c, 5f and 5i, respectively. Three figures are sketched in the same scale for comparison convenience. There are three important points regarding these results: 1) in all three conditions, the beam penetrates through the graphene layer and interacts with the Cu substrate; 2) both the interaction volume and penetration depth increases with the beam voltage; 3) the surface area from which SEs are collected are comparable for 550 V and 1000 V beam energies, but are much larger for a 2000 V beam.

Because graphene films are ultra-thin, low voltage SEM imaging is essential for high resolution surface details. This is because as the beam voltage is reduced, more SEs collected from a surface area defined by the beam spot size. At 1000 V and below, the spatial resolution for most materials is defined
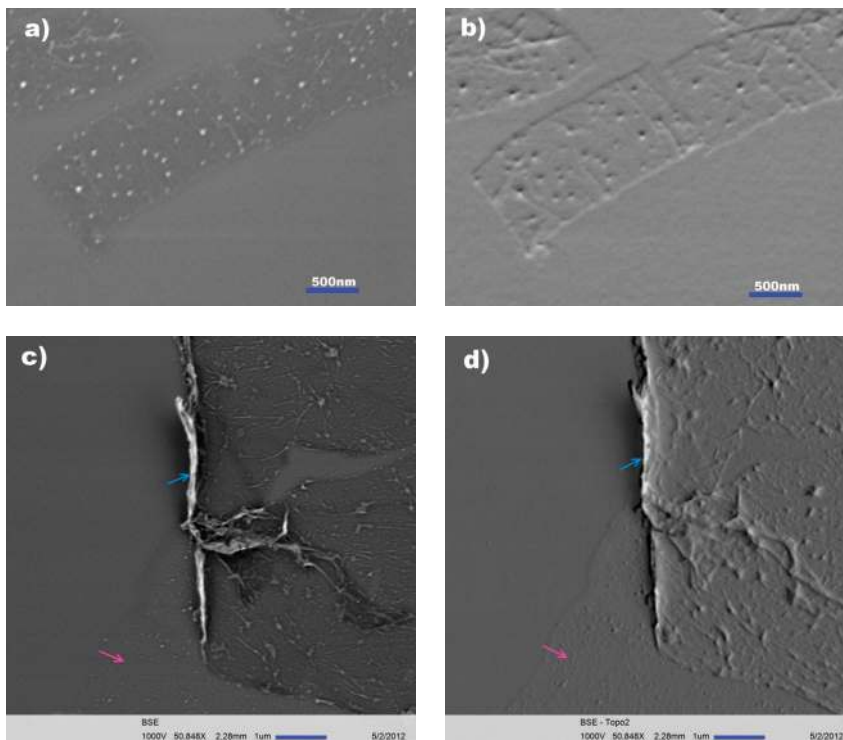

Figure 4. a) SE image of a graphene ribbon showing nanoparticles on its surface; b) topo image reveals more surface details; c) SE image showing formation of a graphene nanoscroll at the edge of a film; d) corresponding topo image of the nanoscroll.
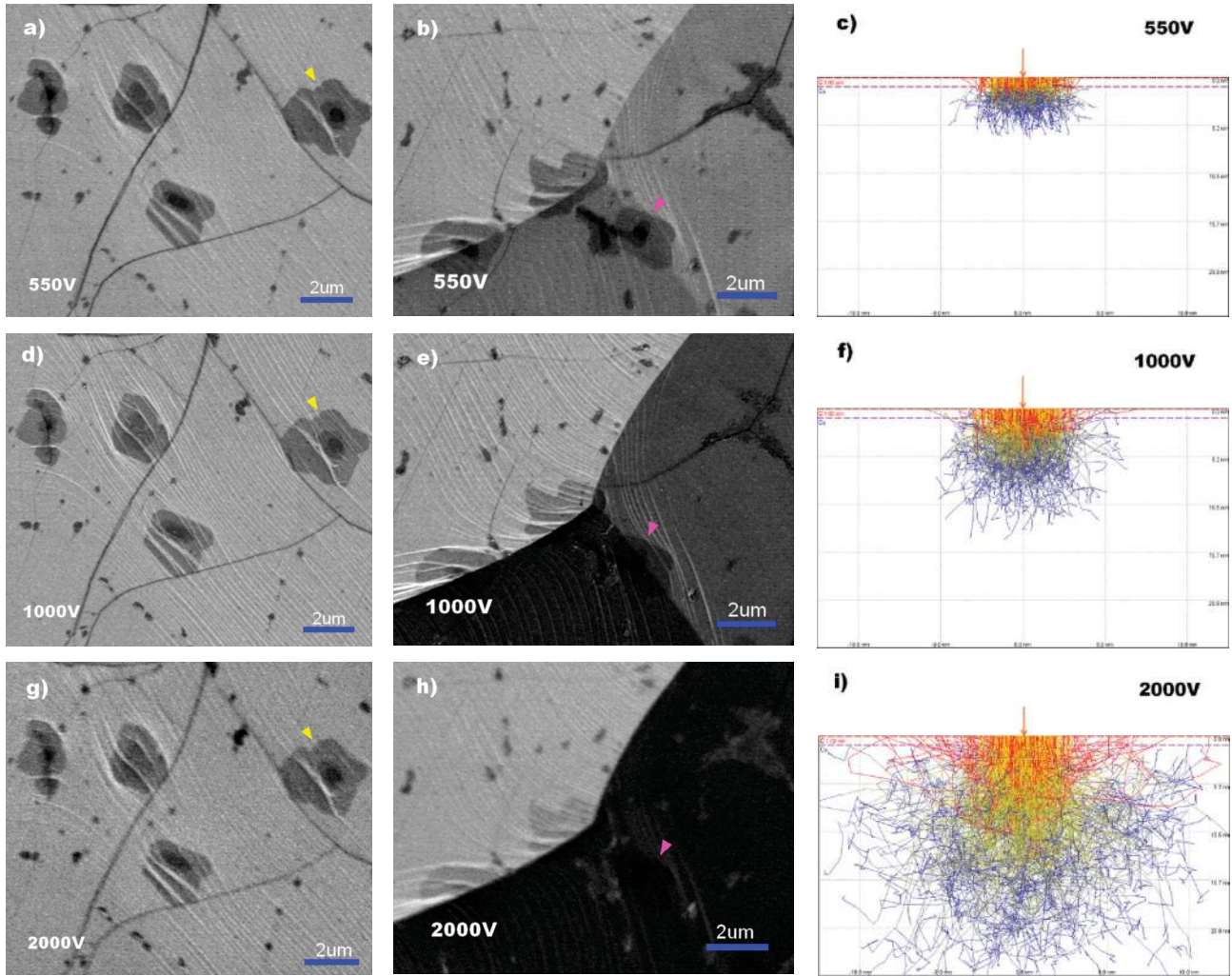
Figure 5. SE images and Monte Carlo simulation results showing the effect of beam voltage on graphene imaging. a–b) images obtained with 550 V of beam voltage; c) simulation result showing a 550 V beam/specimen interaction; d–e) images at 1000 V of beam voltage; f) simulation result for a 1000 V beam; g–h) images at 2000 V of beam voltage; i) simulation result for a 2000 V beam.

by the beam spot size. In principle, imaging graphene on Cu without any beam interaction with the Cu is possible if the energy of used electron beam is sufficiently low. In this case, only information about the surface morphology of the graphene film will be collected. Unfortunately, lens aberrations and increasing sensitivity to external factors like vibration and electromagnetic interference (EMI) will cause the resolution to degrade. Previous work has indicated that imaging at 1000 V is optimal for a few-layer graphene and is independent of the substrate [21]. In this study we found that working with a 1000 V beam seems ideal for identification of different numbers of graphene layers due to the enhanced surface contrast.

Effect of Nonconducting Substrates

In order to fully take advantage of the extraordinary electrical properties of graphene, transferring graphene from metal substrates to insulator substrates is a critical step for realizing electronic applications. After transfer, the non-conducting substrates will affect graphene imaging. SEM imaging at voltages above 3 kV can result in charging effects that make imaging graphene films on non-conducting samples challenging [21]. Scanning with an electron beam at a low energy is expected to overcome this charging problem because the total charge

injected into the sample is close of zero and, in fact, can be tuned by varying the beam voltage so that there is zero charge accumulation.

Here we show some LV FE-SEM images of graphene films on three non-conducting substrates. For comparison, graphene films were transferred using the same technique. Images shown in Figure 6a-c show graphene transferred to a MgO substrate. A cracked area was located to show the contrast between the graphene film and the substrate. The area covered with graphene is darker in color than the bare MgO substrate, as shown in the left top area of Figure 6a. It is not easy to differentiate multi-layer domains on the graphene film which are indicated in cyan circles. Apparently, the MgO
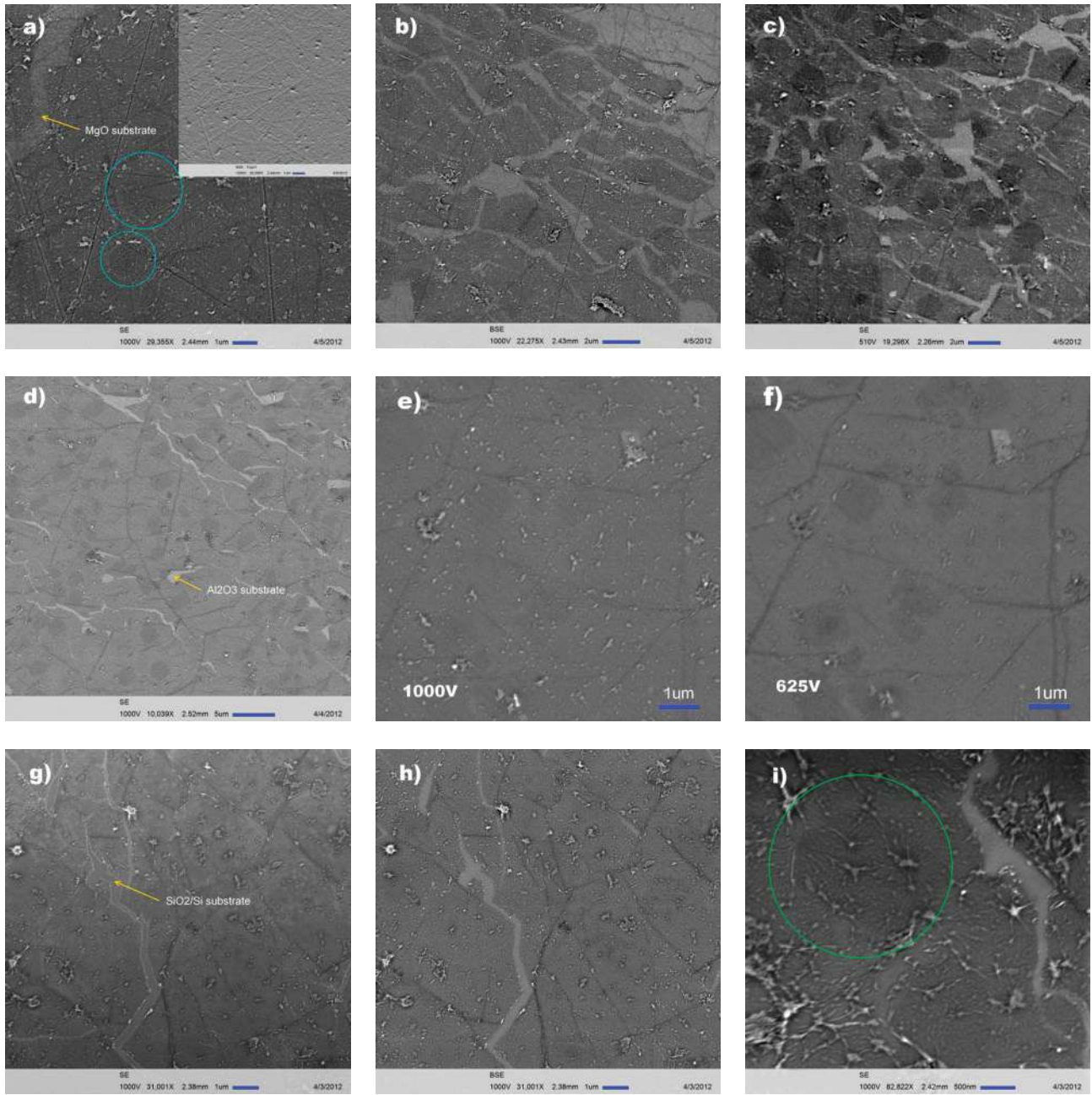
Figure 6. a–c) images of transferred graphene on a rough MgO substrate; d–f) images of transferred graphene on Al$_2$O$_3$ substrate; g–i) images of transferred graphene on a SiO$_2$/Si substrate.

substrate has a very rough surface with a large number of scratches. Compared with the SE image, the topo image (the inset) does not display the edge of graphene film. This can be explained as the topographic features of graphene edge are overwhelmed by the rough MgO surface. Severe charging from the MgO substrate was observed, especially at slow scanning speeds or at high magnifications. Figure 6b is a BSE image showing discontinuous graphene film on the MgO surface. BSE imaging can significantly reduce the charging because the high energy backscattered electrons are less sensitive to charging than secondary electrons. Here a similar resolution was obtained from BSE imaging. At low voltages, the electron beam generates a small interaction volume and the collected SEs and BSEs come from the same region in the sample. Hence BSE imaging at low voltages does not significantly affect the resolution. This is not the case for high voltage imaging. Another option to control the charging effect is to tune the beam voltage to minimize the total charge injected into the sample. For most samples, this means lowering the beam voltage. The SE image shown in Figure 6c was obtained using a 510 V beam. No charging was observed, and a better contrast from multi-layer domains was seen.

In the case of graphene transferred to an Al$_2$O$_3$ substrate, charging was not observed at 1000 V. The transferred graphene film is smooth and multi-layer domains are evident (Figure 6d).

Compared with the image obtained at 1000 V (Figure 6e), Figure 6f obtained at 625 V displays those multi-layer domain more obviously with an enhanced contrast. Figure 6g and 6h are SE image and BSE image of transferred graphene on a SiO_2/Si substrate, respectively. Graphene wrinkles can be seen from both images. Compared with the SE image, the BSE image displays a brighter SiO_2 substrate which can be explained as the charge accumulation on the substrate surface. The image at a higher magnification (Figure 6i) not only reveals a corrugated morphology of the graphene film but also shows multi-layer domains clearly, as indicated by a green circle.

Figure 6a-6i reveal a remarkable difference in graphene morphology after transferred to different substrates by the same method. This preliminary study implies a distinct dependence of graphene film's quality on the properties of the substrates to be transferred such as surface roughness, hydrophilicity, crystallinity, conductivity and others. Further work is needed to fully understand the morphology change of graphene films during the transfer process.

References

[1] K.S. Novoselov, A.K. Geim, S.V. Morozov, D. Jiang, Y. Zhang, S.V. Dubonos, I.V. Grigorieva and A.A. Firsov, Science 306, 666 (2004).

[2] A.K. Geim and K.S. Novoselov, Nature Materials 6, 183 (2007).

[3] X. Du, I. Skachko, A. Barker and E.Y. Andrei, Nature Nanotechnology 3, 491 (2008).

[4] X. Li, Y. Zhu, W. Cai, M. Borysiak, B. Han, D. Chen, R.D. Piner, L. Colombo and R.S. Ruoff, Nano Letters 9, 4359 (2009).

[5] X. Li, W. Cai, J. An, S. Kim, J. Nah, D. Yang, R. Piner, A. Velamakanni, I. Jung, E. Tutuc, S.K. Banerjee, L. Colombo and R.S. Ruoff, Science 324, 1312 (2009).

[6] W. Kochat, A.N. Pal, E.S. Sneha, A. Sampathkumar, A. Gairola, S.A. Chivashankar, S. Raghavan and A. Ghosh, Journal of Applied Physics 110, 014315 (2011).

[7] M. Xu, D. Fujita, J. Gao and N. Hanagata, ACS Nano 4, 2937 (2010).

[8] I. Vlassiouk, M. Regmi, P. Fulvio, S. Dai, P. Datskos, G. Eres and S. Smirnov, ACS Nano 5, 6069 (2011).

[9] K. Yan, H. Peng, Y. Zhou, H. Li and Z. Liu, Nano Letters 11, 1106 (2011).

[10] C.A. Howsare, X. Weng, V. Bojan, D. Snyder and J.A. Robinson, Nanotechnology 23, 135601 (2012).

[11] A. Ismach, C. Druzgalski, S. Penwell, A. Schwrtzberg, M. Zheng, A. Javey, J. Bokor and Y. Zhang, Nano Letters 10, 1542 (2010).

[12] P.-Y. Teng, C.-C. Lu, K. Akiyama-Hasegawa, Y.-C. Lin, C.-H. Yeh, K. Suenaga and P.-W. Chiu, Nano Letters 12, 1379 (2012).

[13] W. Zhu, C. Dimitrakopoulos, M. Freitag and P. Avouris, IEEE Transactions on Nanotechnology 10, 1196 (2011).

[14] M.H. Rümmeli, A. Bachmatiuk, A. Scott, F. Börrnert, J.H. Warner, V. Hoffman, J.-H. Lin, G. Cuniberti, and B. Büchner, ACS Nano 4, 4206 (2010).

[15] K.S. Kim, Y. Zhao, H. Jang, S.Y. Lee, J.M. Kim, K.S. Kim, J.-H. Ahn, P. Kim, J.-Y. Choi and B.H. Hong, Nature 457, 706 (2009).

[16] X. Liang, B.A. Sperling, I. Calizo, G. Cheng, C.A. Hacker, Q. Zhang, Y. Obeng, K. Yan, H. Peng, Q. Li, X. Zhu, H. Yuan, A.R. Hight Walker, Z. Liu, L. Peng and C.A. Richter, ACS Nano 5, 9144 (2011).

[17] X. Li, X. Wang, L. Zhang, S. Lee and H. Dai, Science 319, 1229 (2008).

[18] X. Xie, L. Ju, X. Feng, Y. Sun, R. Zhou, K. Liu, S. Fan, Q. Li and K. Jiang, Nano Letters 9, 2565 (2009).

[19] S.F. Braga, V.R. Coluci, S.B. Legoas, R. Giro, D.S. Galvao and R.H. Baughman, Nano Letters 4, 881 (2004).

[20] D. Drouin, A.R. Couture, D. Joly, X. Tastet, V. Aimez and R. Gauvin, Scanning 29, 92 (2007).

[21] H. Hiura, H. Miyazaki and K. Tsukagoshi, Applied Physics Express 3, 095101 (2010).

[22] J.K. Hite, M.E. Twigg, J.L. Tedesco, A.L. Friedman, R.L. Myers-Ward, C.R. Eddy Jr. and D.K. Gaskill, Nano Letters 11, 1190 (2011).

Summary

In this note, the excellent imaging capability of low voltage field emission scanning electron microscopy for morphology investigation of graphene was demonstrated. Images reveal nanosized surface details on graphene films with an enhanced contrast. This imaging technique offers a fast, non-invasive and effective approach for graphene multi-layer domain identification and film defect detection.

Acknowledgement

Nanomeasurement Systems from Keysight

Keysight Technologies, the premier measurement company, offers high-precision, modular nanomeasurement solutions for research, industry, and education. Exceptional worldwide support is provided by experienced application scientists and technical service personnel. Keysight's leading-edge R&D laboratories ensure the continued, timely introduction and optimization of innovative, easy-to-use nanomeasure system technologies.

www.keysight.com/find/nano

KEYSIGHT
TECHNOLOGIES